THE JOURNAL OF BIOLOGICAL CHEMISTRY VOL. 288, NO. 38, pp. 27059–27067, September 20, 2013

Comparison of the Inhibition Mechanisms of Adalimumab and Infliximab in Treating Tumor Necrosis Factor α-Associated Diseases from a Molecular View*

Received for publication, June 14, 2013, and in revised form, July 15, 2013 Published, JBC Papers in Press, August 13, 2013, DOI 10.1074/jbc.M113.491530

Shi Hu[‡§1], Shuaiyi Liang[‡1], Huaizu Guo[§¶‖], Dapeng Zhang[§¶‖], Hui Li[‖], Xiaoze Wang[**], Weili Yang[**], Weizhu Qian[§¶‖], Sheng Hou[§¶‖], Hao Wang[§¶‖], Yajun Guo[§¶‖2], and Zhiyong Lou[‡3]**

*From the [‡]Laboratory of Structural Biology and Ministry of Education Laboratory of Protein Science, School of Medicine, Tsinghua University, Beijing 100084, China, the [§]International Joint Cancer Institute, Second Military Medical University, Shanghai 200433, China, the [¶]National Engineering Research Center for Antibody Medicine and Shanghai Key Laboratory of Cell Engineering & Antibody, Shanghai 201203, China, the [‖]People's Liberation Army (PLA) General Hospital Cancer Center, PLA Postgraduate School of Medicine, Beijing 100853, China, and the **School of Medicine, Nankai University, Tianjin 300071, China*

Background: The epitope and the TNFα inhabitation mechanism of Adalimumab remain unclear.
Results: The crystal structure of the TNFα in complex with Adalimumab is reported at a resolution of 3.1 Å.
Conclusion: The epitope of Adalimumab provided information that Adalimumab may have clinical advantage compared with Infliximab.
Significance: These data reveal the Adalimumab's mechanism of TNFα inhibition and its advantages compared with other TNF inhibitors in clinical practice.

TNFα-targeting therapy with the use of the drugs Etanercept, Infliximab, and Adalimumab is used in the clinical treatment of various inflammatory and immune diseases. Although all of these reagents function to disrupt the interaction between TNFα and its receptors, clinical investigations showed the advantages of Adalimumab treatment compared with Etanercept and Infliximab. However, the underlying molecular mechanism of action of Adalimumab remains unclear. In our previous work, we presented structural data on how Infliximab binds with the E-F loop of TNFα and functions as a TNFα receptor-binding blocker. To further elucidate the variations between TNFα inhibitors, we solved the crystal structure of TNFα in complex with Adalimumab Fab. The structural observation and the mutagenesis analysis provided direct evidence for identifying the Adalimumab epitope on TNFα and revealed the mechanism of Adalimumab inhibition of TNFα by occupying the TNFα receptor-binding site. The larger antigen-antibody interface in TNFα Adalimumab also provided information at a molecular level for further understanding the clinical advantages of Adalimumab therapy compared with Infliximab.

TNF is an immunity-modulating cytokine required for immune processes. The unregulated activities of TNFs can lead to the development of inflammatory diseases. Excess amounts of TNFα expressed in cells are associated with the development of immune diseases, including rheumatoid arthritis, Crohn's disease, psoriatic arthritis, and inflammatory bowel disease (1, 2). The function of TNFα requires smooth interaction with its two receptors, TNF receptor 1 (TNFR1)[4] and TNF receptor 2 (TNFR2). Blocking the interaction between TNFα and TNFRs has successfully been developed as a therapy in treating inflammatory or autoimmune diseases (3, 4). TNFα neutralization therapies, including the use of a soluble TNFR2-Fc recombinant (Etanercept), a mouse-human chimera mAb (Infliximab), or a human mAb (Adalimumab), have been introduced in the past decades for the management of rheumatoid arthritis and other immune diseases (5).

Although all of these TNFα blockers function by interrupting the TNFα-TNFR interaction, information on whether the different TNFα inhibitors have similar clinical efficacy remains controversial because of the lack of randomized clinical trial meta-analyses. In the early stages of clinical usage of Infliximab, its discontinuation was reported to result in loss of response. This largely affected patients who received long term treatment and later discontinued use (6). Approximately 10% of the patients discontinued the use Infliximab because of the loss of response. The discontinued use caused remissions, representing an additional 13% of patients. This practice pattern still occurs, but the frequency of Infliximab discontinuation in present day clinical practice is considerably lower because of the enhanced understanding that drug holidays may lead to loss of efficacy, attenuation of response, and acute and delayed hypersensitivity reactions through retreatment (7). A longitudinal

* This work was supported by 973 Project Grants 2010CB833600, 2013CB911103, 2012CB724500, and 2010CB735605; National Natural Science Foundation of China Grants 31170678 and 31000332; Key Projects in the Tianjin Science and Technology Pillar Program Grant 10ZCKFSY08800; and 2011 Science and Technology Innovation Fund Grant 11C26211203971.
The atomic coordinates and structure factors (code 3WD5) have been deposited in the Protein Data Bank (http://wwpdb.org/).
[1] Both authors contributed equally to this work.
[2] To whom correspondence may be addressed: International Joint Cancer Institute, Second Military Medical University, Shanghai 200433, China. Tel.: 86-21-81880701; Fax: 86-21-81880701; E-mail: yjguo@smmu.edu.cn.
[3] To whom correspondence may be addressed: Laboratory of Structural Biology, New Life Science Bldg., Tsinghua University, Beijing 100084, China. Tel.: 86-10-62771493; Fax: 86-10-62773145; E-mail: louzy@xtal.tsinghua.edu.cn.

[4] The abbreviations used are: TNFR1, TNF receptor 1; CRD, cysteine-rich domain; CDR, complementarity-determining region.

study involving 93 Crohn's disease patients was performed to compare the effectiveness of Infliximab and Adalimumab. The study suggested that no obvious differences could be found in obtaining and maintaining remission (8). Another study drew a similar conclusion, claiming that the difference between Infliximab and Adalimumab is not obvious because the long term maintenance of the clinical remission between the two antibodies and their effectiveness are similar in both primary and secondary-tertiary centers (9). However, evidence from a Dutch observational study involving 770 patients with rheumatoid arthritis suggested that more patients achieve moderate responses to Adalimumab and Etanercept compared with Infliximab, but the potential baseline biases corrected for in the Dutch study were not specified, and strict response criteria were not included (10). Another study also directly compared the treatment responses, remission rates, and drug adherence in patients with rheumatoid arthritis treated with Adalimumab, Etanercept, or Infliximab using the nationwide DANBIO registry, which has been designed to capture operational clinical data as part of routine clinical care. The results showed that Adalimumab had the highest rates in treatment response and disease remission compared with the other two TNFα inhibitors (11). Furthermore, a very recent study implemented a matching adjusted indirect comparison technique, showing that Adalimumab is associated with the higher American College of Rheumatology 70% improvement criteria and Psoriasis Area and Severity Index 50/75/90 response rates compared with Etanercept at week 24 and a higher American College of Rheumatology 70% improvement criteria response rate than that of Infliximab at week 14 (12). These clinical investigations suggested that Adalimumab is more advantageous in TNFα-blocking therapy of autoimmune diseases.

However, the underlying inhibition mechanisms of these TNF blockers with regard to clinical efficacy remain elusive. In particular, no reports have compared the binding epitopes of these drugs that have been widely used, despite the fact that the affinity and the epitope are the crucial elements in evaluating antibody drugs. In a previous work, we reported the crystal structure of the TNFα-Infliximab Fab complex, presenting the inhibition mechanism of Infliximab of the TNFα–TNFR interaction through partial overlap with the TNFα-TNFR interface. We also revealed the pivotal role of the E-F loop of TNFα in Infliximab recognition (5). To further elucidate the inhibition mechanism of Adalimumab, in particular the variation on the mechanism of Infliximab and Adalimumab targeting at the TNFα-TNFR contact, we launched a crystallographic and mutagenesis analysis on the TNFα-Adalimumab Fab complex.

EXPERIMENTAL PROCEDURES

Protein Expression, Purification, and Characterization—Residues 77–233 of human TNFα followed by a His_6 tag were expressed in *Escherichia coli* BL21 (DE3) cells (Novagen) using the pET-22b(+) vector (Novagen). The cells were grown in LB medium at 37 °C until the A_{600} reached 0.6–0.8, and the expression of the protein was induced with 0.5 mM isopropyl β-D-thiogalactopyranoside for 4 h. The cells were incubated in PBS containing 20 mM phosphate (pH 8.0) and 150 mM NaCl with an additional 1 mg/ml lysozyme, 1 mM PMSF, and 1% Triton X-100 for 20 min on ice and then sonicated. The cell lysate was removed through centrifugation (10,000 × *g*) and filtration (0.45 μm). Solid ammonium sulfate was added to the supernatant at a 35% final concentration and was immediately mixed and incubated on a roller at 4 °C for 2 h. The precipitant was discarded, and solid ammonium sulfate was continuously added to the supernatant until a final concentration of 60% was achieved. The concentration was immediately mixed and incubated on a roller at 4 °C for 4 h. The precipitated protein was pelleted through centrifugation, and then the supernatant was discarded. The precipitant was dissolved in PBS buffer and separated through gel filtration using a Superdex 75 column (GE Healthcare). The precipitant was desalted to 20 mM Tris-HCl (pH 8.0), and the target fraction was further purified with a 20-column volume linear NaCl gradient elution from a high performance Q-Sepharose (GE Healthcare). The purity was confirmed to be >95% through SDS-PAGE analysis. The bioactivity was measured through a cytotoxicity assay using the TNF-susceptible murine L-929 cell line in the presence of the metabolic inhibitor actinomycin D, as described in Ref. 13.

Adalimumab was cloned, expressed, and purified following reported procedures. EcoRV and XbaI sites were added to the 5′-end of the heavy chain variable region gene (V_H), and an NheI site was added to the 3′-end. The PCR product was cloned into the pGEM-T vector, and the sequence of the product was confirmed through DNA sequencing. V_H was excised through EcoRV and NheI digestion and then inserted into the EcoRV/NheI sites of the pAH4604 vector containing the human gamma-1 constant region gene (C_H). The resultant pAH4604-V_H vector was cleaved with XbaI and BamHI. The 3.3-kb fragment containing the human antibody heavy chain gene was cloned into the pcDNA3.1(−) vector (Invitrogen), which was digested with the same restriction enzymes and yielded the heavy chain expression vector pcDNA3.1(−)V_HC_H. The human κ chain constant cDNA (C_L) was obtained as a 0.3-kb PCR product derived from pAG4622. The light chain variable region gene (V_L) of Adalimumab was fused to the 5′-end of C_L through the overlapping PCR method. The resultant human light chain gene (V_LC_L), which has a HindIII site upstream of the start codon and an EcoRI site downstream of the stop codon, was cloned into the pGEM-T vector. The sequence of the chain was then verified. V_LC_L was excised through HindIII and EcoRI digestion and was ligated into pcDNA3.1 The Zeo(+) vector (Invitrogen) cleaved with the same restriction enzymes yielded the chimeric light chain expression vector pcDNA3.1 Zeo(+)V_LC_L. The light and heavy chain expression vectors were co-transfected into Chinese hamster ovary K1 cells using Lipofectamine 2000 (Invitrogen). The stable transfectants were isolated through limiting dilution in the presence of 600 μg/ml G418 and 300 μg/ml Zeocin. The culture supernatants from the individual cell clones were analyzed for antibody production through a sandwich enzyme-linked immunosorbent assay. The assay used goat anti-human IgG Fc (KPL, Gaithersburg, MD) as the capture antibody and goat anti-human κ-HRP (Southern Biotechnology Associates, Birmingham, AL) as the detecting antibody. Purified human IgG1/κ (Sigma) was used as the standard control. The clones producing the highest amount of recombinant antibody were selected and grown in serum-free

medium. The recombinant antibodies were purified through protein A affinity chromatography from the serum-free culture supernatant. The antibody concentrations were determined by absorbance at 280 nm, and the purity was confirmed through SDS-PAGE analysis. Bioactivity was measured in a cytotoxicity antagonist assay using the TNF-susceptible murine L-929 cell line in the presence of the metabolic inhibitors actinomycin D and TNFα.

The Fab fragment of Adalimumab for the crystallographic investigation was obtained through papain digestion of the antibody. The digested protein sample was loaded onto a Protein A-Sepharose 4 FF column (GE Healthcare). The Fab fragment eluted in the flow through was separated from the Fc fragment and further purified through ion exchange chromatography using a Q-Sepharose FF column (GE Healthcare). The protein sample was concentrated to ~10 mg/ml and then exchanged to a stock buffer containing 10 mM Tris-HCl (pH 8.0) and 100 mM NaCl. TNFα was subsequently mixed with an excess of Adalimumab Fab, and the complex was purified through gel filtration chromatography (GE Healthcare). This complex was dialyzed against 50 mM Tris-HCl (pH 8.0) and 150 mM NaCl and was concentrated to 30 mg/ml.

Crystallization—Crystallization was performed at 291 K through the hanging drop vapor diffusion technique. The crystals were obtained by mixing 1 μl of the protein solution with an equal volume of a reservoir solution. The mixture drop was equilibrated against 500 μl of the reservoir solution. The crystals were obtained with a reservoir solution containing 30% PEG 400, 0.1 M sodium acetate trihydrate (pH 4.6), and 0.1 M cadmium chloride hydrate, which reached the final dimensions of $100 \times 100 \times 100\ \mu m^3$ with the best diffraction within 1 week. The crystals were then cryo-protected through soaking in a cryo-protectant composed of the reservoir solution and 5% glycol. The cryo-protected crystals were subsequently flash-cooled in liquid nitrogen and then transferred into a dry nitrogen stream at 100 K for x-ray data collection.

X-ray Data Collection, Processing, and Structure Determination—The diffraction data for the TNFα-Adalimumab Fab complex were collected at Beamline BL17A (Photon Factory) with a resolution of 3.1 Å. The data were processed, integrated, and scaled using the HKL2000 package (14). The crystals belong to space group $I2_13$ with cell parameters $a = b = c = 161.8$ Å, $\alpha = \beta = \gamma = 90°$. The statistics of all data collections and structure refinements are summarized in Table 1.

The TNFα-Adalimumab Fab structure was solved through the molecular replacement method, which employs the crystal structures of apo TNFα (Protein Data Bank code 1TNF) and GA101 Fab (Protein Data Bank code 3PP3) as the initial searching model using the program PHASER (15). The clear solutions in both the rotation and translation functions indicated the presence of one complex molecule, including one TNFα and one Adalimumab Fab molecule, in one asymmetric unit. This result is consistent with the Matthews coefficient and solvent content (16). The inconsistent residues were manually rebuilt in the program Coot (17) under the guidance of the $F_o - F_c$ and $2F_o - F_c$ electron density maps. The residues were refined in PHENIX (18), and the respective working R_{factor} and R_{free} values decreased from 0.42 and 0.48 to 0.19 and 0.28, respectively, for all data from 50.0 to 3.1 Å. The refinement was monitored by calculating R_{free} based on a subset containing 5% of the total reflections. Model geometry was verified using the program PROCHECK (19). The data collection and refinement statistics are presented in detail in Table 1. All structure figures were prepared using PyMOL (20).

TABLE 1
Data collection and refinement statistics

Parameters	TNFα-Humira Fab complex
Data collection statistics	
Cell parameters	$a = b = c = 161.8$ Å, $\alpha = \beta = \gamma = 90°$
Space group	$I2_13$
Wavelength used (Å)	1.0000
Resolution (Å)	50.0 (3.2)-3.1[c]
No. of all reflections	226,799 (11,466)
No. of unique reflections	24,923 (1274)
Completeness (%)	100.0 (100.0)
Average $I/\sigma(I)$	8.0 (5.1)
R_{merge} (%)[a]	17.2 (64.3)
Refinement statistics	
No. of reflections used ($\sigma(F) > 0$)	12,943
R_{work} (%)[b]	18.67
R_{free} (%)[b]	27.50
Root mean square deviation bond distance (Å)	0.010
Root mean square deviation bond angle (°)	1.412
Average overall B value (Å^2)	48.2
Ramachandran plot (excluding Pro and Gly)	
Residues in most favored regions	504 (88.3%)
Residues in additionally allowed regions	42 (7.4%)

[a] $R_{merge} = \Sigma_h\Sigma_i|I_{ih} - \langle I_h\rangle|/\Sigma_h\Sigma_i\langle I_h\rangle$, where $\langle I_h\rangle$ is the mean of multiple observations, I_{ih}, of a given reflection h.
[b] $R_{work} = \Sigma||F_p(obs) - |F_p(calc)||/\Sigma|F_p(obs)|$; R_{free} is an R factor for a selected subset (5%) of reflections that was not included in prior refinement calculations.
[c] The numbers in parentheses are corresponding values for the highest resolution shell (2.5–2.4 Å).

Kinetics and Affinity Assay of TNFα Mutants—Site-directed mutants ($_{TNF}$P20A, $_{TNF}$Q21A, $_{TNF}$E23A, $_{TNF}$K65A, $_{TNF}$Q67A $_{TNF}$T72A, $_{TNF}$K90A, $_{TNF}$V91A, $_{TNF}$N92A, $_{TNF}$E110A, $_{TNF}$P113A, $_{TNF}$E135A, $_{TNF}$I136A, and $_{TNF}$E146A) were created through PCR. The mutants were expressed and purified as recommended for wild-type proteins. Adalimumab Fab was immobilized on the surface of a CM-5 sensor chip (GE Healthcare) through amine coupling following the manufacturer's instructions. The maximal electrostatic interaction was obtained with 10 mM sodium acetate (pH 5.0). We regularly obtained Adalimumab Fab immobilization levels ranging from ~1000 to 1500 resonance units. The BIAcore T100 (GE Healthcare) instrument for the binding experiments was operated at 25 °C, and the assay buffer was PBS. The contact time (the period during which the analyte consisting of TNFα mutants 4 and 11 was perfused over the chip) was limited to 300 s. The flow rate was set at 30 μl/min. A 10 mM glycine (pH 2.0) solution was used to dissociate the bound TNF at the end of each experiment while retaining the surface integrity for chip surface regeneration.

RESULTS

Structure of the TNFα-Adalimumab Fab Complex—The TNFα-Adalimumab Fab complex was crystallized, and the structure was determined and refined to 3.1 Å resolution with a final R_{work} value of 19.7% ($R_{free} = 28.5\%$) (Table 1). One TNFα-Adalimumab Fab complex molecule in the asymmetric unit with a Matthews coefficient of 3.5 Å^3/Da exists, corresponding to 64% of the solvent content (21). The central TNFα trimer is

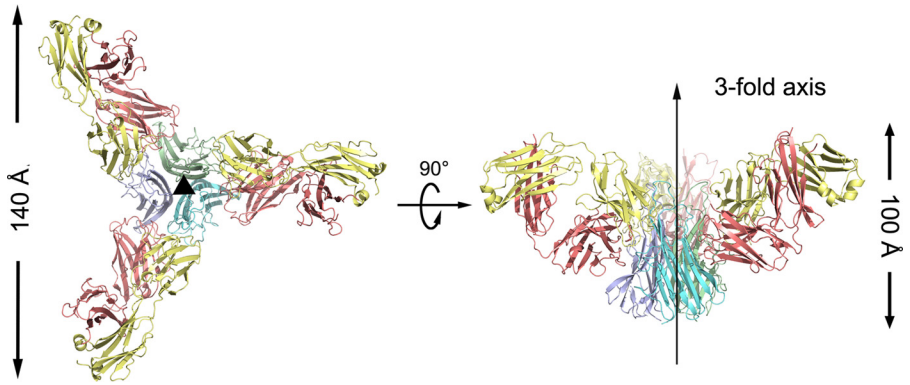

FIGURE 1. **Overall structure of the TNFα-Adalimumab Fab complex.** The TNFα-Adalimumab Fab complex is shown as ribbon diagrams in two orientations: *top view*, looking down the crystallographic 3-fold symmetry axis; *side view*, with the crystallographic 3-fold axis vertical (*middle*). The central TNFα molecules are colored *green*, *blue*, and *cyan*, respectively; the light chain and heavy chain of the Adalimumab Fab are colored *yellow* and *red*, respectively.

bound by three symmetrically arranged Adalimumab Fab molecules related through a crystallographic 3-fold axis (Fig. 1), which is analogous to the structures of TNFα-TNFR2 (22), TNFβ-TNFR1 (23), and TNFα in complex with other binding partners (5, 24).

Superimposing TNFα in the TNFα-Adalimumab Fab complex with its free form yielded a root mean square deviation of 0.9 Å for all of the Cα atoms, indicating that no significant overall structural difference occurred, except for several key residues on the antibody-antigen interface (Fig. 2). Residues $_{TNF}$Leu-29, $_{TNF}$Arg-31, $_{TNF}$Ser-52, and $_{TNF}$Tyr-56, which are crucial for TNFα cytotoxicity and TNFR interaction (25), were confirmed to have the correct conformation through a cytotoxicity assay.

The Adalimumab Fab presents a canonical β-sandwich immunoglobulin fold with the heavy chain folding into the V_H and C_H domains and the light chain folding into the V_L and C_L domains. The elbow angle, defined as the subtended angle by two pseudo 2-fold axes relating V_H to V_L and C_H to C_L of Adalimumab Fab, was ~140°. The complementarity-determining region (CDR) loops L1, L2, L3, H1, and H2 of Adalimumab belong to the Chothia canonical classes (26) 2, 1, 1, 1, and 3, respectively. The CDR loops L1, L2, L3, H1, H2, and H3 of Adalimumab form a large deep pocket to accommodate the epitope (Fig. 3), whereas not all of the CDR loops of Infliximab participate in the interaction with TNFα (5).

Interactions between TNFα and Adalimumab—The Adalimumab Fab binds to TNFα through a large and highly complementary interface, with a total buried surface area of 2,540 Å^2 (Fig. 3*A*), which is consistent with the high avid association between Adalimumab and TNFα (27). The Adalimumab epitope on TNFα is composed of a number of discontinuous segments, including residues $_{TNF}$Pro-19, $_{TNF}$Gln-20, $_{TNF}$Glu-23, $_{TNF}$Lys-65 to $_{TNF}$Gln-67, $_{TNF}$Glu-10 to $_{TNF}$Pro-113, $_{TNF}$Tyr-141, and $_{TNF}$Ala-145, to $_{TNF}$Glu-146 and $_{TNF}$Thr-71, $_{TNF}$His-72, $_{TNF}$Thr-77, $_{TNF}$Thr-79, $_{TNF}$Ser-81, $_{TNF}$Lys-89 to $_{TNF}$Asn-91, and $_{TNF}$Glu-135 to $_{TNF}$Asn-137 of an adjacent TNFα protomer (Figs. 3 and 4). Both the heavy and light chains of Adalimumab participated in the interaction with TNFα, with all of the contacts coming from CDRs. CDRs L2 and H2 contribute to the majority of the interactions with the antigen. Additional contributions are given from CDRs L1, L3, H1, and H3. Over 20 pairs of hydrogen bonds or salt bridges stabilized the TNFα-Adalimumab Fab complex (Table 2), which indicates a strong and stable interface within this antigen-antibody pair.

FIGURE 2. **Structural variations of TNFα in free form and complex forms.** A single subunit of the TNFα trimer in the free form or complex forms of the TNFα-Infliximab Fab, the Adalimumab Fab, and TNFR2 are shown. The free state of the TNFα molecule is colored *orange*, whereas complex states with Infliximab Fab, Adalimumab Fab, and TNFR2 are colored *pale green*, *red*, and *light blue*, respectively.

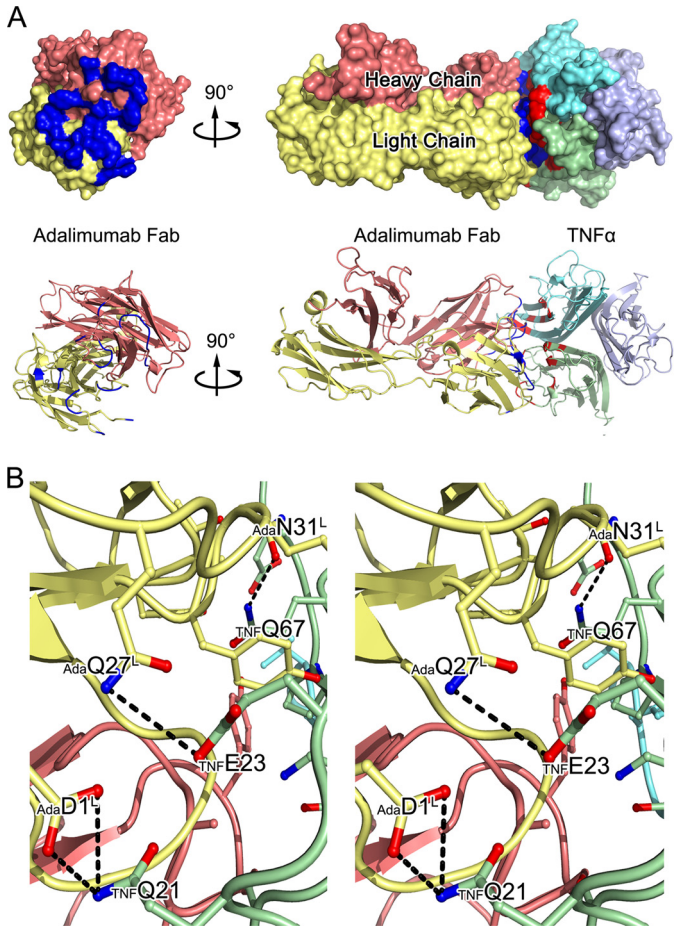

FIGURE 3. **The TNFα-Adalimumab Fab interface.** *A*, surface representations of the Adalimumab Fab (*left*) and the TNFα-Adalimumab Fab complex (*right*) and ribbon diagrams corresponding to the surfaces shown above with the same color scheme. The light chain and heavy chains of the Adalimumab Fab are colored *yellow* and *red*, respectively, whereas TNFα molecules are colored *green*, *blue*, and *cyan*. Contact surfaces are highlighted in *blue* on Adalimumab and *red* on TNFα. *B*, stereo view of the detailed TNFα-Adalimumab Fab interface. The residues that are involved in the intermolecular interaction are shown as *colored sticks* with the same scheme as the surface representation above; the Adalimumab Fab and TNFα molecules are presented as ribbon diagrams. *Dashed lines* denote hydrogen bonds.

The light chain of Adalimumab interacts with strands A and C, as well as the A-A′ and the E-F loops of TNFα. Residues $_{Ada}$Asp-1 and $_{Ada}$Arg-93 of CDR L3 form three hydrogen bonds and a salt bridge with $_{TNF}$Pro-20, $_{TNF}$Gln-21, and $_{TNF}$Glu-23 at the beginning of strand A and the A-A′ loop of TNFα. An extensive network of intermolecular side chain hydrogen bonds between CDR L1 and strand C of TNFα contributes to most of the light chain interactions and positions the side chain of $_{Ada}$Arg-30, $_{Ada}$Asn-31, and $_{Ada}$Tyr-32 of CDR L1 interacting with $_{TNF}$Lys-65 and $_{TNF}$Gln-67 of TNFα. CDR L2 additionally contributes to the antigen-antibody communication through the hydrogen bond formed by the side chain of $_{Ada}$Thr-53 with the residue $_{TNF}$Ala-111 on the E-F loop of TNFα.

The interface between the heavy chain of Adalimumab and TNFα is primarily composed of the residues in the G-H loop, several amino acids in strand D, and the D-E loop of an adjacent TNFα protomer. $_{Ada}$His-57 in CDR H2 and $_{Ada}$Ser-103 and $_{Ada}$Thr-104 in CDR H3 make hydrogen bonds with $_{TNF}$Ala-145 to $_{TNF}$Ser-147 in the G-H loop. Moreover, the residues $_{Ada}$Asn-54 and $_{Ada}$Gly-56 of CDR H2 contact $_{TNF}$Thr-79, $_{TNF}$Ser-81, and $_{TNF}$Asn-92 in strands D and E and $_{TNF}$Glu-135 in strand G of another neighboring TNFα polypeptide.

Comparison of the Interfaces between TNFα and TNFRs and the Infliximab Fab and the Adalimumab Fab—A comparison of the interfaces in TNFα-TNFRs, TNFα-Infliximab, and TNFα-Adalimumab Fab provides a better understanding of the mechanism of TNFα inhibition by blocking the communication with TNFRs, which is what allows Adalimumab to effectively inhibit the TNFα function more directly compared with Infliximab (Fig. 5).

In the TNFα-TNFR2 complex, one TNFR2 molecule interacts with two adjacent TNFα protomers, such as in the TNFα-Adalimumab complex. By contrast, the antigen-antibody interaction only involves one TNFα molecule in the TNFα-Infliximab complex (5). The structures of the extracellular domains of the TNFR superfamily are composed of cysteine-rich domains (CRDs) that typically contain six cysteine residues that form three disulfide bonds (23). In the TNFα-TNFR2 complex, the CRD2 and CRD3 of TNFR2 play important roles in the cytokine-receptor interaction. CRD2 and CRD3 contact strand A, the A-A′ loop, and the G-H loop of one TNFα protomer and generate several hydrogen bonds with strand D, the D-E loop, E-F loop, and the G-H loop of a neighboring TNFα molecule. These contacts greatly overlap with the TNFα-Adalimumab interface, in which strand D, strand E, strand G, the E-F loop, and the G-H loop of TNFα have important roles. By contrast, a different subset of the secondary structures of TNFα, including strand C, strand D, strand G, the C-D loop and E-F loop, interacts with Infliximab.

Residues $_{TNFR}$Asp-58, $_{TNFR}$Ser-59, $_{TNFR}$Gln-63, $_{TNFR}$Trp-67, $_{TNFR}$Glu-70, $_{TNFR}$Cys-71, $_{TNFR}$Cys-74, $_{TNFR}$Ser-76, $_{TNFR}$Arg-77 of CRD2, $_{TNFR}$Tyr-103, $_{TNFR}$Gln-109, and $_{TNFR}$Arg-113 of CRD3 in TNFR2, as well as $_{TNF}$Gln-21, $_{TNF}$Gln-23, $_{TNF}$Arg-32, $_{TNF}$Ala-33, $_{TNF}$His-73, $_{TNF}$Ser-86, $_{TNF}$Tyr-87, $_{TNF}$Pro-113, $_{TNF}$Tyr-115, $_{TNF}$Asp-143, $_{TNF}$Phe-144, $_{TNF}$Ala-145, $_{TNF}$Glu-146, and $_{TNF}$Gln-149 of TNFα, participate and greatly contribute to these interactions in the cytokine-receptor interface. Among them, $_{TNF}$Gln-21 in strand A, $_{TNF}$Gln-23 in the A-A′ loop, $_{TNF}$His-73 in strand D, $_{TNF}$Pro-113 and $_{TNF}$Tyr-115 in the E-F loop, and $_{TNF}$Ala-145 and $_{TNF}$Gln-146 in the G-H loop have considerably important roles in both the interface of the TNFα-TNFR2 complex and the TNFα-Adalimumab complex, whereas none of these residues can be observed in the TNFα-Infliximab structure. Additionally, the Infliximab paratope consists of five CDRs, namely L2, L3, H1, H2, and H3, whereas the Adalimumab paratope is composed of all six CDRs (Fig. 6).

These structural features reveal that the Adalimumab epitope directly overlaps the TNFR binding area with a larger area of the antigen-antibody interface of TNFα-Adalimumab (2,340 Å^2), whereas the Infliximab epitope is distant from the receptor-binding sites with less interacting surface (1,977 Å^2).

Structure-based Mutagenesis Study on the Antigen-Antibody Interface—We identified 14 selected TNFα residues for mutagenesis analysis, including $_{TNF}$Pro-20, $_{TNF}$Gln-21, $_{TNF}$Glu-23, $_{TNF}$Lys-65, $_{TNF}$Gln-67, $_{TNF}$Lys-72, $_{TNF}$Lys-90, $_{TNF}$Val-91, $_{TNF}$Asn-92, $_{TNF}$Glu-110, $_{TNF}$Pro-113, $_{TNF}$Glu-135, $_{TNF}$Ile-136 and $_{TNF}$Glu-146 (Table 2), according to the structural information of the

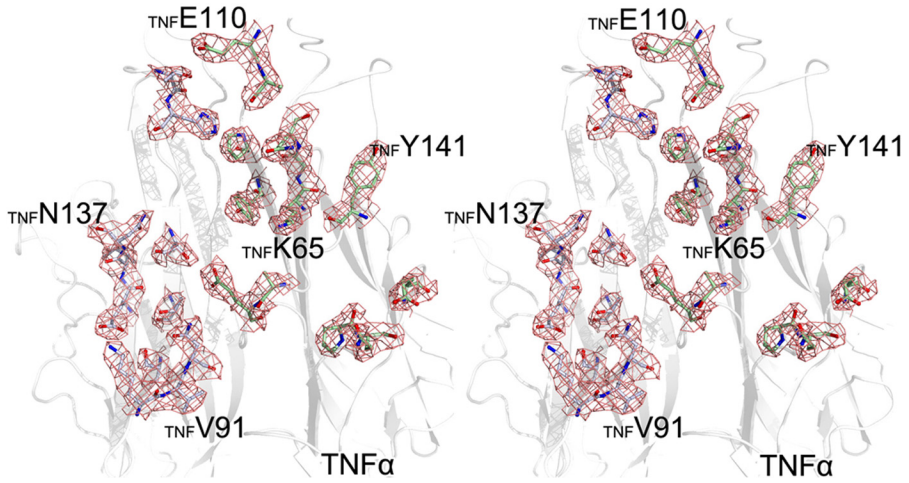

FIGURE 4. **A stereo view of the epitope density map in the TNFα-Adalimumab Fab binding interface.** The omit map of the epitope on the TNFα polypeptide is contoured at 1.0 σ. The TNFα molecule is shown as a *white cartoon*, whereas the epitope is represented as *colored sticks*.

TABLE 2
Complete list of interactions between TNFα and the Adalimumab Fab (≤3.6 Å)

TNFα		Adalimumab Fab			
Residue	Atom	Residue	Atom	CDR loop	Distance
					Å
Gln-67	C^{δ}	Ile-56$_H$	$C^{\delta1}$	H2	3.04
	$O^{\epsilon1}$	Ile-56$_H$	$C^{\delta1}$		2.82
	$N^{\epsilon2}$	Ile-56$_H$	$C^{\delta1}$		3.18
	$N^{\epsilon2}$	Ser-53$_H$	O^{γ}		3.58
	$N^{\epsilon2}$	Ser-55$_H$	O^{γ}		3.44
Pro-70	C^{β}	Ser-105$_H$	O^{γ}	H3	3.46
	C^{β}	Tyr-50$_L$	OH	L2	3.45
	C^{β}	Ser-105$_H$	C^{β}	H3	3.57
	C^{γ}	Tyr-103$_H$	O	H3	3.03
Ser-71	C^{β}	Tyr-50$_L$	$C^{\epsilon1}$	L2	3.25
	C^{β}		C^{ζ}	L2	3.34
His-73	C^{β}	Tyr-50$_L$	$C^{\delta2}$	L2	3.50
Thr-105	O	Tyr-102$_H$	OH	H3	2.86
Glu-107	N	Tyr-102$_H$	OH	H3	3.58
	C^{α}		OH	H3	3.53
	C^{β}		OH	H3	3.51
Ala-109	O	Tyr-103$_H$	OH	H3	3.22
Glu-110	C^{β}	Asn-31$_H$	$N^{\delta2}$	H2	3.53
Asn-137	O	Trp-94$_L$	N	L3	2.92
		Ser-93$_L$	C^{α}		3.30
		Ser-93$_L$	O^{γ}		3.55
Asn-137	C^{β}	Ser-93$_L$	O^{γ}	L3	3.48
	C^{γ}	His-92$_L$	O		3.58
	$N^{\delta2}$	His-92$_L$	O		2.81
	$N^{\delta2}$	His-92$_L$	$C^{\epsilon1}$		3.54
	$N^{\delta2}$	His-92$_L$	$N^{\epsilon2}$		3.43
Arg-138	C^{δ}	His-92$_L$	O	L3	3.28
	NH1	Ser-91$_L$	O		3.44
Asp-140	$O^{\delta1}$	Trp-94$_L$	C^{β}	L3	3.52
	$O^{\delta1}$	Trp-94$_L$	C^{γ}	L3	3.56
	$O^{\delta2}$	Arg-52$_H$	C^{ζ}	H2	3.58
	$O^{\delta2}$	Arg-52$_H$	$N^{\theta1}$	H2	3.27
	$O^{\delta2}$	Arg-52$_H$	$N^{\theta2}$	H2	3.00
Tyr-141	$C^{\epsilon1}$	Arg-52$_H$	$N^{\theta1}$	H2	3.43
	OH	Trp-33$_H$	$C^{\theta2}$	H1	3.35

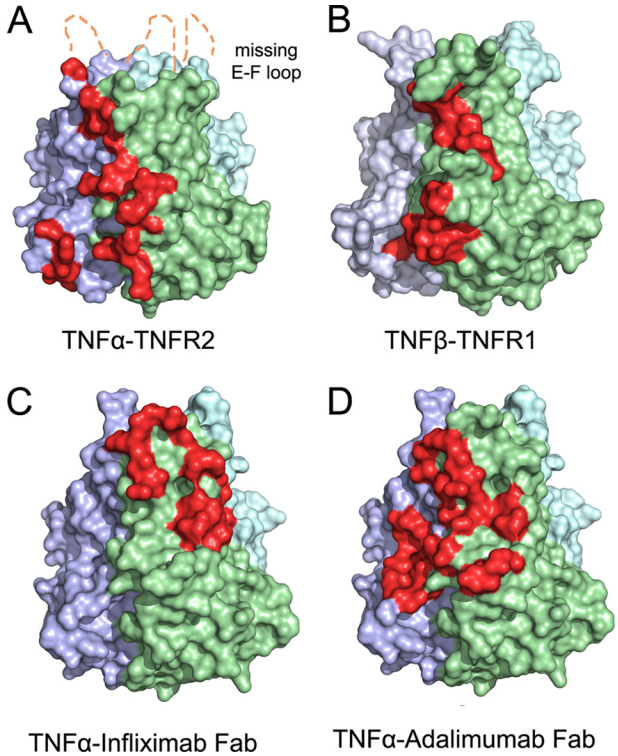

FIGURE 5. **A comparison of the interface between TNFα and receptors and Infliximab/Adalimumab Fab complexes.** A comparison of the interface between TNFα and receptors and mAbs is shown. TNFα from the complex structures is represented as a colored surface with TNFR2 and the mAb Fabs interface highlighted in *red* at one of three interfaces on the TNFα trimer. The E-F loop region, which is missing in the TNFα-TNFR2 (*A*) complex because of a lack of interaction, is labeled. The TNFβ from the TNFβ-TNFR1 (*B*) complex structure is shown as a colored surface with one of the TNFR1-binding sites highlighted in *red*. The TNFα-Infliximab Fab (*C*) and the TNFα-Adalimumab Fab (*D*) interfaces are shown as colored surfaces with TNFα-binding sites highlighted in *red*.

TNFα-Adalimumab Fab. We substituted each residue with alanine and measured the binding affinities with Adalimumab through surface plasmon resonance to study the effects of these residues on the TNFα-Adalimumab interaction (Table 3).

The replacement of $_{TNF}$Pro-21, $_{TNF}$Thr-72, $_{TNF}$Lys-90, $_{TNF}$Val-91, $_{TNF}$Glu-110, and $_{TNF}$Ile-136 with alanine residues did not obviously affect the binding capacity of TNFα with Adalimumab, whereas the substitutions on $_{TNF}$Glu-23, $_{TNF}$Asn-92, and $_{TNF}$Pro-113 showed 5–10-fold decreases in binding. Notably, the mutant $_{TNF}$Q21A presented a sharp decrease in the binding to Adalimumab with a 200-fold lower binding affinity. The same phenomenon was observed in the $_{TNF}$K65A, $_{TNF}$Q67A, $_{TNF}$E135A, and $_{TNF}$E146A mutations. All of these mutants resulted in a 100–200-fold affinity decrease. The $_{TNF}$Gln-21 of strand A, $_{TNF}$Lys-65 and $_{TNF}$Gln-67 of strand C, as well as $_{TNF}$Glu-135 and $_{TNF}$Glu-146 of the G-H loop, which are crucial for TNFα-

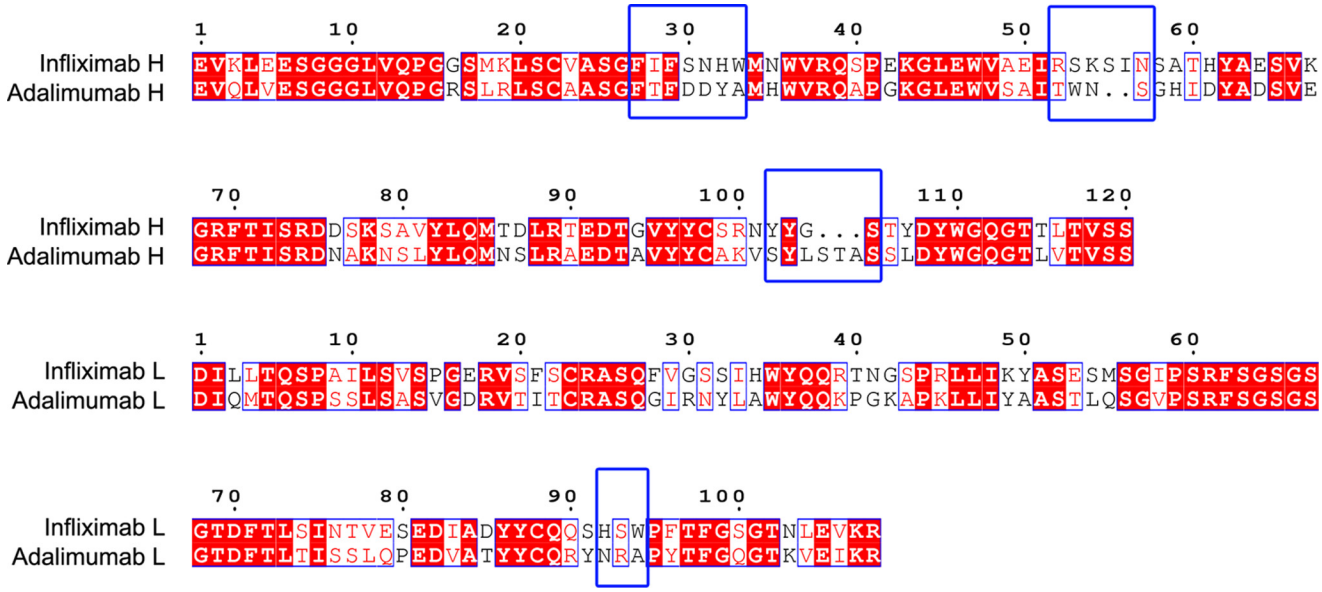

FIGURE 6. **Sequence comparison between two TNFα therapeutic antibodies (Infliximab and Adalimumab).** The CDRs are highlighted by *black frames* and labeled. The residues that play crucial roles in the antibody-antigen interaction are framed with *blue frames*. The residue numbers (*top*) refer to those in Infliximab.

TABLE 3

Kinetics and binding affinity of TNFα mutants with the Adalimumab Fab

Kinetics and affinity of TNFα mutant and the Adalimumab Fab were analyzed using a BIAcore T100. Wild type TNFα and the mutants were passed over the immobilized Adalimumab Fab surface, and the data were globally analyzed using a simultaneous fit for both dissociation (k_d) and association (k_a). The value for K_D was calculated as k_d/k_a.

	k_a	k_d	K_D
	$M^{-1}\cdot s^{-1}$	s^{-1}	M
WT TNFα	$4.784 \pm 0.717 \times 10^{5}$	$5.512 \pm 0.826 \times 10^{-5}$	$1.152 \pm 0.172 \times 10^{-10}$
$_{TNF}$P20A	$3.785 \pm 0.567 \times 10^{5}$	$8.491 \pm 1.273 \times 10^{-5}$	$2.244 \pm 0.336 \times 10^{-10}$
$_{TNF}$Q21A	$2.286 \pm 0.342 \times 10^{4}$	$5.338 \pm 0.801 \times 10^{-4}$	$2.335 \pm 0.350 \times 10^{-8}$
$_{TNF}$E23A	$2.665 \pm 0.399 \times 10^{5}$	$3.886 \pm 0.582 \times 10^{-4}$	$1.458 \pm 0.218 \times 10^{-9}$
$_{TNF}$K65A	$3.211 \pm 0.481 \times 10^{4}$	$4.339 \pm 0.650 \times 10^{-4}$	$1.351 \pm 0.202 \times 10^{-8}$
$_{TNF}$Q67A	$2.557 \pm 3.383 \times 10^{4}$	$5.087 \pm 0.763 \times 10^{-4}$	$1.989 \pm 0.298 \times 10^{-8}$
$_{TNF}$T72A	$4.778 \pm 0.716 \times 10^{5}$	$5.033 \pm 0.755 \times 10^{-5}$	$1.053 \pm 0.157 \times 10^{-10}$
$_{TNF}$K90A	$3.956 \pm 0.593 \times 10^{5}$	$3.893 \pm 0.583 \times 10^{-4}$	$9.841 \pm 1.476 \times 10^{-10}$
$_{TNF}$V91A	$1.159 \pm 0.173 \times 10^{5}$	$8.496 \pm 1.274 \times 10^{-5}$	$5.593 \pm 0.838 \times 10^{-10}$
$_{TNF}$N92A	$2.554 \pm 0.383 \times 10^{5}$	$5.223 \pm 0.783 \times 10^{-4}$	$2.045 \pm 0.306 \times 10^{-9}$
$_{TNF}$E110A	$2.144 \pm 0.321 \times 10^{5}$	$2.967 \pm 0.445 \times 10^{-5}$	$1.384 \pm 0.207 \times 10^{-10}$
$_{TNF}$P113A	$1.187 \pm 0.178 \times 10^{6}$	$1.394 \pm 0.209 \times 10^{3}$	$1.175 \pm 0.176 \times 10^{-9}$
$_{TNF}$E135A	$2.493 \pm 0.373 \times 10^{4}$	$2.948 \pm 0.442 \times 10^{-4}$	$1.183 \pm 0.177 \times 10^{-8}$
$_{TNF}$I136A	$4.666 \pm 0.699 \times 10^{5}$	$5.133 \pm 0.769 \times 10^{-5}$	$1.100 \pm 0.165 \times 10^{-10}$
$_{TNF}$E146A	$2.337 \pm 0.350 \times 10^{4}$	$4.223 \pm 0.633 \times 10^{-4}$	$1.808 \pm 0.271 \times 10^{-8}$

Adalimumab interaction, also play key roles in TNFα-TNFR2 communication (22).

DISCUSSION

Etanercept, Infliximab, and Adalimumab have remarkably enhanced the treatment of immune diseases after they were successfully developed. A number of clinical investigations have studied the current use of these TNFα inhibitors and revealed that Adalimumab has an advantage in therapeutic treatment. However, the cause for this distinct efficacy remains elusive, although all of these TNFα inhibitors function as blockers that interrupt TNFα-TNFR communication.

Because Etanercept is a soluble TNFR2-Fc recombinant, the structure of TNFα-TNFR2 explains the mechanism by which Etanercept blocks the TNFα-TNFR interaction by occupying the receptor binding site on TNFα (22). One Etanercept/TNFR2 molecule interacted with two TNFα molecules, and the majority of the interface was made up of CRD2 and CRD3 regions of Etanercept/TNFR2 and the interface of two adjacent TNFα protomers, with a buried surface of 2,500 Å^2 (22) (Fig. 5*A*). The epitope of Infliximab on TNFα is primarily composed of C-D and E-F loop residues and several key residues in strands C and D of the TNFα molecule, with a total buried surface of 1,977 Å^2 (Fig. 5*C*). Interestingly, one Infliximab Fab contacts only one TNFα protomer, whereas two adjacent TNFα protomers both contribute to the Etanercept/TNFR2 contact. Although both Etanercept and Infliximab bind to TNFα, their affinity for binding to TNFα is controversial. Scallon *et al.* (28) suggested that Infliximab has a slightly lower K_D value of 4.5×10^{-10} M compared with 1.15×10^{-9} M for Etanercept. However, Smith *et al.* (29) showed greater affinity of Etanercept with a K_D of 2.35×10^{-11} M compared with the lower K_D value of 1.17×10^{-10} M of Infliximab. The larger affinity displayed by Infliximab is believed to be a consequence of the greater stability of the TNFα-Infliximab complex (28), whereas the greater affinity of Etanercept was attributed to the faster rate of ligand binding (29). The area of buried surfaces

shown in the structural information is likely consistent with the greater K_D value of Etanercept.

Although the binding affinities displayed by Etanercept and Infliximab are debated, Adalimumab has been reported to bind TNFα with a relatively higher affinity than Etanercept and Infliximab, with K_D values ranging from 7.05×10^{-11} M (30) to 1.0×10^{-10} M (31). The buried surface of one Adalimumab Fab with trimeric TNFα is consistently 2,536 Å^2, which is larger than those of one Infliximab Fab and one Etanercept molecule with trimeric TNFα. The structural comparisons of the TNFα-Adalimumab Fab with the TNFα-Infliximab and TNFα-TNFR2 complex reveal that the Adalimumab epitope extensively overlaps with the TNFα-TNFR2 interface, whereas Infliximab only partially occupies the TNFα-TNFR2 binding area and is mainly targeted at the E-F loop of TNFα and spatially obstructs the correct interaction with TNFRs. Furthermore, a total of 7 of 21 TNFα residues involved in TNFR2 binding also participate in contacting the Adalimumab Fab. The three regions, including residues $_{TNF}$Gln-21, $_{TNF}$Glu-23, $_{TNF}$Ala-145, and $_{TNF}$Glu-146 that form two negatively charged surface patches, residues $_{TNF}$Pro-113 and $_{TNF}$Tyr-115 that form a hydrophobic surface patch and residues $_{TNF}$Val-85–$_{TNF}$Tyr-87 and $_{TNF}$Thr-89 of an adjacent TNFα that also form a negatively charged surface patch, are shared by both TNFR2 and Adalimumab Fab. Notably, although $_{TNF}$Gln-21, $_{TNF}$Glu-23, $_{TNF}$His-73, $_{TNF}$Pro-113, $_{TNF}$Tyr-115, $_{TNF}$Ala-145, and $_{TNF}$Gln-146 play essential roles in the TNFR2 and Adalimumab interaction, they are irrelevant for TNFα-Infliximab recognition. In the previous investigations, random mutagenesis studies on TNFα were performed to produce inactive molecules that lost their cytotoxic activity. Interestingly, the residues that were identified to lose most cytotoxic activity are involved in both TNFR2 and Adalimumab interactions. For example, the activity of TNFα dropped when alterations were introduced in $_{TNF}$Glu-23, $_{TNF}$Pro-113, and $_{TNF}$Tyr-115 without marked changes in immunoreactivity or physicochemical characteristics, as well as $_{TNF}$Q146K mutation, which causes a nearly complete loss of the cytotoxicity for TNFα (32). Moreover, $_{TNF}$Asp-143, $_{TNF}$Gln-149, and $_{TNF}$Glu-24, which are important residues for the TNFR2 recognition not only in the structure analysis but also in previous mutagenesis studies (22, 32, 33), are involved in the TNFα-Adalimumab interface.

In early stage usage of Infliximab, a number of patients discontinued the use of Infliximab because of the loss of response (6). It was proposed that Infliximab is a chimeric mAb, and its usage in humans could lead to the production of "antibodies to Infliximab" in a small subset of patients (34–37). Using more human sequence content by grafting murine CDRs may be crucial for the integral capacity of antigen binding and should be retained during humanization (38). Although this practice pattern still occurs, in present day clinical practice, the frequency of Infliximab discontinuation for this reason is low (7). However, the efficacy of Adalimumab-based TNF-blocking therapy in autoimmune diseases is higher than that of Etanercept and Infliximab. The structure shown here illustrates how Adalimumab prevents ligands from binding to TNFR2, inhibits ligand-receptor binding, and blocks TNFR activation. The primary consequence of Adalimumab binding to TNFα is the steric blocking of TNFα and the prevention of ligand binding to the receptor. The solvent-accessible surface contributed by the ligand-receptor interaction covers over 60% of the total interface between TNFα and the Adalimumab Fab, which indicates a straightforward overlap between the TNFα receptor binding sites and the Adalimumab epitope. Moreover, several residues that are crucial for TNFα receptor binding also participate in the TNFα-Adalimumab Fab interface, especially the groove between the two associated TNFα molecules in the TNFα trimer. These results may partly explain the clinical data regarding the more significant effectiveness of the treatment compared with placebo in inducing remission in patients with Crohn's disease who are intolerant of or have lost response to Infliximab. Therefore, binding Adalimumab to TNFα can efficiently compete with binding TNFRs to TNFα. The interface between TNFα and TNFRs is blocked in the presence of a sufficient amount of Adalimumab, which prevents the function of TNFα in the pathological process. Taken together, these data indicate that Adalimumab occupies the binding site and competitively inhibits the binding of TNFR to TNFα. Combined with the structural information of TNFα-Infliximab, these structures provide information to improve the interface complementarity between antibody and antigen, to strengthen the interaction, and to thereby enhance the binding affinity through altering the paratope of the antibody in targeted therapy and antibody engineering. Moreover, this information may also be useful to evaluate the antibody in the early stages of use. A therapeutic antibody whose epitope directly occupies the receptor binding position and competitively inhibits TNFR-TNFα communication, such as Adalimumab, may have better and more predictable clinical effects than an antibody that has a more distant epitope and uses the steric properties, such as Infliximab. Once a new antibody is identified as having promising results in preclinical studies, a crystallography study to determine its precise epitope may help us in making strategic decisions before proceeding with costly clinical drug trials.

In summary, our findings structurally explain the varying clinical observations for the anti-TNF antibodies. An evaluation of the effectiveness showed that Adalimumab had better outcomes than Infliximab from a molecular view. This finding, which agrees with another clinical report (10), highlights an opportunity for therapeutic improvement despite the significant advances in the past decade. The precise epitope revealed by our complex structure provides useful information for structure-based improvements for current TNFα mAbs and highlights the importance of identifying the predictors of a beneficial outcome through the structural and biological characteristics of the drug.

Acknowledgments—We thank the staffs of Photon Factory, Japan Synchrotron Radiation Facility, and Beijing Synchrotron Radiation Facility for generous help in collecting x-ray data.

REFERENCES

1. Shealy, D. J., and Visvanathan, S. (2008) Anti-TNF antibodies. Lessons from the past, roadmap for the future. *Handb. Exp. Pharmacol.* **181,** 101–129
2. Palladino, M. A., Bahjat, F. R., Theodorakis, E. A., and Moldawer, L. L. (2003) Anti-TNF-α therapies: the next generation. *Nat. Rev. Drug Discov.*

2, 736–746
3. Aggarwal, B. B. (2003) Signalling pathways of the TNF superfamily. A double-edged sword. *Nat. Rev. Immunol.* **3,** 745–756
4. Tansey, M. G., and Szymkowski, D. E. (2009) The TNF superfamily in 2009. New pathways, new indications, and new drugs. *Drug Discov. Today* **14,** 1082–1088
5. Liang, S., Dai, J., Hou, S., Su, L., Zhang, D., Guo, H., Hu, S., Wang, H., Rao, Z., Guo, Y., and Lou, Z. (2013) Structural basis for treating tumor necrosis factor α (TNFα)-associated diseases with the therapeutic antibody Infliximab. *J. Biol. Chem.* **288,** 13799–13807
6. Schnitzler, F., Fidder, H., Ferrante, M., Noman, M., Arijs, I., Van Assche, G., Hoffman, I., Van Steen, K., Vermeire, S., and Rutgeerts, P. (2009) Long-term outcome of treatment with Infliximab in 614 patients with Crohn's disease. Results from a single-centre cohort. *Gut* **58,** 492–500
7. Seminerio, J. L., Loftus, E. V., Jr., Colombel, J. F., Thapa, P., and Sandborn, W. J. (2013) Infliximab for Crohn's disease. The first 500 patients followed up through 2009. *Dig. Dis. Sci.* **58,** 797–806
8. Zorzi, F., Zuzzi, S., Onali, S., Calabrese, E., Condino, G., Petruzziello, C., Ascolani, M., Pallone, F., and Biancone, L. (2012) Efficacy and safety of Infliximab and Adalimumab in Crohn's disease. A single centre study. *Aliment. Pharmacol. Ther.* **35,** 1397–1407
9. Tursi, A., Elisei, W., Picchio, M., and Penna, A. (2013) Letter. Are Infliximab and Adalimumab similar for Crohn's disease in clinical practice? *Aliment. Pharmacol. Ther.* **37,** 763–764
10. Kievit, W., Adang, E. M., Fransen, J., Kuper, H. H., van de Laar, M. A., Jansen, T. L., De Gendt, C. M., De Rooij, D. J., Brus, H. L., Van Oijen, P. C., and Van Riel, P. C. (2008) The effectiveness and medication costs of three anti-tumour necrosis factor α agents in the treatment of rheumatoid arthritis from prospective clinical practice data. *Ann. Rheum. Dis.* **67,** 1229–1234
11. Hetland, M. L., Christensen, I. J., Tarp, U., Dreyer, L., Hansen, A., Hansen, I. T., Kollerup, G., Linde, L., Lindegaard, H. M., Poulsen, U. E., Schlemmer, A., Jensen, D. V., Jensen, S., Hostenkamp, G., and Østergaard, M. (2010) Direct comparison of treatment responses, remission rates, and drug adherence in patients with rheumatoid arthritis treated with Adalimumab, Etanercept, or Infliximab. Results from eight years of surveillance of clinical practice in the nationwide Danish DANBIO registry. *Arthritis Rheum.* **62,** 22–32
12. Kirson, N. Y., Rao, S., Birnbaum, H. G., Kantor, E., Wei, R. S., and Cifaldi, M. (2013) Matching-adjusted indirect comparison of Adalimumab *vs.* Etanercept and Infliximab for the treatment of psoriatic arthritis. *J. Med. Econ.* **16,** 479–489
13. Matthews, N., and Neale, M. L. (1987) *Lymphokines and Interferons: A Practical Approach*, p. 296, IRL Press, London
14. Otwinowski, Z., and Minor, W. (1997) Processing of x-ray diffraction data collected in oscillation mode, in *Macromolecular Crystallography: Part A* (Carter, C. W., Jr., and Sweet, R. M., eds) pp. 307–326, Academic Press, Orlando, FL
15. McCoy, A. J., Grosse-Kunstleve, R. W., Storoni, L. C., and Read, R. J. (2005) Likelihood-enhanced fast translation functions. *Acta Crystallogr. D* **61,** 458–464
16. Matthews, B. W. (1968) Solvent content of protein crystals. *J. Mol. Biol.* **33,** 491–497
17. Emsley, P., and Cowtan, K. (2004) Coot. Model-building tools for molecular graphics. *Acta Crystallogr. D Biol. Crystallogr.* **60,** 2126–2132
18. Adams, P. D., Grosse-Kunstleve, R. W., Hung, L. W., Ioerger, T. R., McCoy, A. J., Moriarty, N. W., Read, R. J., Sacchettini, J. C., Sauter, N. K., and Terwilliger, T. C. (2002) PHENIX. Building new software for automated crystallographic structure determination. *Acta Crystallogr. D Biol. Crystallogr.* **58,** 1948–1954
19. Laskowski, R., MacArthur, M., Moss, D., and Thornton, J. (1993) PROCHECK: a program to check the stereochemical quality of protein structures. *J. Appl. Crystallogr.* **26,** 283–291
20. DeLano, W. L. (2002) The PyMOL Molecular Graphics System, Schrödinger, LLC, New York
21. Collaborative Computational Project, Number 4 (1994) The CCP4 suite. Programs for protein crystallography. *Acta Crystallogr. D Biol. Crystallogr.* **50,** 760–763
22. Mukai, Y., Nakamura, T., Yoshikawa, M., Yoshioka, Y., Tsunoda, S., Nakagawa, S., Yamagata, Y., and Tsutsumi, Y. (2010) Solution of the structure of the TNF-TNFR2 complex. *Sci. Signal.* **3,** ra83
23. Banner, D. W., D'Arcy, A., Janes, W., Gentz, R., Schoenfeld, H. J., Broger, C., Loetscher, H., and Lesslauer, W. (1993) Crystal structure of the soluble human 55 kd TNF receptor-human TNFβ complex. Implications for TNF receptor activation. *Cell* **73,** 431–445
24. Yang, Z., West, A. P., Jr., and Bjorkman, P. J. (2009) Crystal structure of TNFα complexed with a poxvirus MHC-related TNF binding protein. *Nat. Struct. Mol. Biol.* **16,** 1189–1191
25. Idriss, H. T., and Naismith, J. H. (2000) TNFα and the TNF receptor superfamily. Structure-function relationship(s). *Microsc. Res. Tech.* **50,** 184–195
26. Al-Lazikani, B., Lesk, A. M., and Chothia, C. (1997) Standard conformations for the canonical structures of immunoglobulins. *J. Mol. Biol.* **273,** 927–948
27. Kaymakcalan, Z., Sakorafas, P., Bose, S., Scesney, S., Xiong, L., Hanzatian, D. K., Salfeld, J., and Sasso, E. H. (2009) Comparisons of affinities, avidities, and complement activation of Adalimumab, Infliximab, and Etanercept in binding to soluble and membrane tumor necrosis factor. *Clin. Immunol.* **131,** 308–316
28. Scallon, B., Cai, A., Solowski, N., Rosenberg, A., Song, X. Y., Shealy, D., and Wagner, C. (2002) Binding and functional comparisons of two types of tumor necrosis factor antagonists. *J. Pharmacol. Exp. Ther.* **301,** 418–426
29. Davis, T., Friend, D., and Smith, C. A. (2002) Comparative TNF binding characteristics of etanercept (Enbrel) and infliximab (Remicade). *Ann. Rheum. Dis.* **61,** 184
30. Granneman, R. G., Zhang, Y., Noertersheuser, P. A., Velagapudi, R. B., Awni, W. M., and Locke, C. S. (2003) Pharmacokinetic/pharmacodynamic (PK/PD) relationships of adalimumab (HumiraTM) in rheumatoid arthritis (RA) patients during phase II/III clinical trials. *Arthritis Rheum.* **48,** S140
31. Santora, L. C., Kaymakcalan, Z., Sakorafas, P., Krull, I. S., and Grant, K. (2001) Characterization of noncovalent complexes of recombinant human monoclonal antibody and antigen using cation exchange, size exclusion chromatography, and BIAcore. *Anal. Biochem.* **299,** 119–129
32. Van Ostade, X., Tavernier, J., and Fiers, W. (1994) Structure-activity studies of human tumour necrosis factors. *Protein Eng.* **7,** 5–22
33. Mukai, Y., Shibata, H., Nakamura, T., Yoshioka, Y., Abe, Y., Nomura, T., Taniai, M., Ohta, T., Ikemizu, S., Nakagawa, S., Tsunoda, S., Kamada, H., Yamagata, Y., and Tsutsumi, Y. (2009) Structure-function relationship of tumor necrosis factor (TNF) and its receptor interaction based on 3D structural analysis of a fully active TNFR1-selective TNF mutant. *J. Mol. Biol.* **385,** 1221–1229
34. Bachmann, F., Nast, A., Sterry, W., and Philipp, S. (2010) Safety and efficacy of the tumor necrosis factor antagonists. *Semin. Cutan. Med. Surg.* **29,** 35–47
35. Alonso-Ruiz, A., Pijoan, J. I., Ansuategui, E., Urkaregi, A., Calabozo, M., and Quintana, A. (2008) Tumor necrosis factor α drugs in rheumatoid arthritis. Systematic review and metaanalysis of efficacy and safety. *BMC Musculoskelet. Disord.* **9,** 52
36. Wiens, A., Venson, R., Correr, C. J., Otuki, M. F., and Pontarolo, R. (2010) Meta-analysis of the efficacy and safety of Adalimumab, Etanercept, and Infliximab for the treatment of rheumatoid arthritis. *Pharmacotherapy* **30,** 339–353
37. Baidoo, L., and Lichtenstein, G. R. (2005) What next after Infliximab? *Am. J. Gastroenterol.* **100,** 80–83
38. Bernett, M. J., Karki, S., Moore, G. L., Leung, I. W., Chen, H., Pong, E., Nguyen, D. H., Jacinto, J., Zalevsky, J., Muchhal, U. S., Desjarlais, J. R., and Lazar, G. A. (2010) Engineering fully human monoclonal antibodies from murine variable regions. *J. Mol. Biol.* **396,** 1474–1490